LEGIBILITY NOTICE

A major purpose of the Technical Information Center is to provide the broadest dissemination possible of information contained in DOE's Research and Development Reports to business, industry, the academic community, and federal, state and local governments.

Although a small portion of this report is not reproducible, it is being made available to expedite the availability of information on the research discussed herein.

LA-UR -87-3170

Los Alamos National Laboratory is operated by the University of California for the United States Department of Energy under contract W-7405-ENG-36

TITLE DEFLAGRATION-TO-DETONATION IN HMX UNDER HIGH CONFINEMENT

LA-UR--87-3170

DE88 000492

AUTHOR(S) J. M. McAfee, A. W. Campbell, and B. W Asay
Los Alamos National Laboratory, M-8

SUBMITTED TO DEA Proceedings, MBB Schrobenhausen, Germany, July 1987

DISCLAIMER

MASTER

Los Alamos Los Alamos National Laboratory
Los Alamos, New Mexico 87545

FORM NO. 836 R4

DEFLAGRATION TO DETONATION IN HMX UNDER HIGH CONFINEMENT

John M. McAfee, A. Wayne Campbell, and Blaine W Asay
Explosives Applications Group, M-8
Los Alamos National Laboratory
P. O. Box 1663, MS J960
Los Alamos, NM 87545

ABSTRACT

The deflagration-to-detonation behavior of HMX confined in steel tubes was studied by means of x radiography, light emission, and various pin techniques. Unlike most reported experiments, the HMX bed was ignited by driving a piston (initially at rest and in contact with the HMX) into the bed with the pressure generated from burning, low-density HMX on the opposite side of the piston. Because a gasless igniter is used to start the burning of the low-density HMX, the piston has a relatively smooth initial motion. Analysis of the data from these experiments gives a rather detailed picture of the DDT process under these conditions.

INTRODUCTION

This is an extension of work reported by Campbell.[1] Because of the complex nature of the deflagration-to-detonation (DDT) process, we simplify the process of igniting HMX in the tube by pushing a combustion-driven piston into the lightly ramped HMX bed. Ideally, this approach separates the early effects of conductive and convective burning from those effects at higher pressure that begin the compaction of the granulated bed. Additionally, this method of DDT initiation removes (to a first approximation) any effect of a hot-gas-producing igniter.

The hypothesis given by Campbell[1] for the steps of DDT is similar to that proposed in this work. However, the mechanism described here is based on more

extensive experimental observation and is more detailed than that of Ref. 1. Note that the deduced mechanism is presented after the experimental description, but before the experimental evidence.

A schematic of the experimental arrangement is given in Figure 1. A maraging steel tube (12.7-mm i.d. and 23.8-mm o.d.) is hand packed with 8-mm layers of Class A HMX. A 0.13-mm-thick Pb foil is placed between each increment of HMX as a radiographic marker. The O-ring sealed piston at the bottom of the tube is driven into the HMX bed by igniting the low-density (≤ 0.5 g/cm^3) HMX in the burn chamber with a combination of a pyrofuse and a stoichiometric mixture of Ti and B. The pressure in the burn chamber is measured with a transducer in the gauge holder. The response of the HMX bed is measured with a combination of diagnostics: self-shorting (capped) pins measure the trajectory of low-pressure waves (2- to7-MPa closing pressure); coaxial ionization pins measure the onset of conductivity; optical fibers and detectors measure light emission; and x radiographs measure the position of the Pb foils. Figure 2 is a photograph of a typical DDT tube.

The chronology of a generic DDT experiment is shown in Figure 3. The initial conditions are the piston at rest, in contact with the 65% of theoretical maximum density (TMD) HMX bed (Figure 3a). The motion of the piston p generates a compaction wave c (Figure 3b) with a velocity of approximately 400 m/s and a density near 90% TMD. Piston velocity increases to the point that the stress of the bed compaction approximately equals the driving pressure. The velocity settles to about 100 m/s after the piston travels a very short distance. Throughout this dynamic compaction of the bed, shear of and friction between the granules provide energy to start combustion in the compacted material near the piston face. The bed, compacted by the piston, is not readily permeated by combustion product gases. Thus, the burning progresses up the tube as a well-defined wave b (Figure 3c).

The burn wave acts as an accelerating piston. With each incremental acceleration, stress waves are launched from the burn front. These stress waves are represented schematically in the distance-vs-time plot in Figure 4. Up the tube from the burn front these stress waves coalesce. When the resultant stress produced is greater than the strength of the 90% TMD HMX, the bed will collapse forming a region of near 100% TMD (Figure 3d). The bottom of this "plug" region is noted in Figure 3 as g. The

top of the plug G moves slowly relative to g until the burn wave impinges on the plug bottom and the pressure rises rapidly. The plug bottom behaves like a second piston driven by the burn region, and it accelerates with increasing pressure. Simple mass conservation shows that the plug grows rapidly in thickness with the top of the plug G moving several times faster than the bottom. The velocities are great enough that the plug top is an accelerating shock (Figure 3e). The transition to detonation occurs when the shock pressure is sufficient for initiation of the 90% compact (Figure 3f). This is regarded as a simple shock-to-detonation transition. The run-to-detonation, commonly denoted by x^*, is analogous with, but not exactly equal to, the plug thickness. The detonation proceeds up the tube at a velocity characteristic of the 90% TMD HMX (D_1 in Figure 4) until it overtakes the original compaction wave c, where the detonation slows to the velocity characteristic of the original 65% TMD bed (D_2 in Figure 4).

RESULTS AND DISCUSSION

The results from the radiographs are typified by those shown in Figure 5 for Shot No. B-9026. The figure consists of radiographs taken at three different times. The first is a static exposure showing the position of the equally spaced Pb foils before the HMX in the burn chamber is lit. The first dynamic shows the piston moving into the tube and the change in spacing of foils 3-6. The second dynamic was taken after the transition to detonation. The detonation wave is between foils 10 and 11. Foils 3-6 continue to be closely spaced, and the tube wall expands slowly in this region.

Quantitative analysis of the foil positions and the tube expansion results in a measure of the average material density between adjacent foils. Typical results of this analysis are shown in Figure 6, where the results of Shot No. B-9153 are interleaved with those of Shot No. B-9026. The salient features of these density-vs-position plots are easily correlated with the schematic in Figure 3. Figure 6 (a) shows the 90% TMD compaction wave as the only feature. This is the situation in Figure 3(b). Figure 6(b) shows a 100% TMD plug between about 33 and 50 mm, with a region of lower density (hotter) from the piston to about 30 mm indicating burning. This corresponds to Figure 3(e). The situation represented in Figures 6 (c-e) is after the transition to detonation,

corresponding to Figure 3(f). The detonation wave is pictured at positions of about 65, 83, and 92 mm, successively, whereas the plug region remains intact in its original position. The low-density burning region continues to heat, as seen from the decrease in density.

The most complete combination of capped and ionization pin data are given in Figure 7 for Shot No. B-9036. These data show conclusive evidence for detonation in compacted material. In Figure 7(a), the combination of capped and ionization pins shows the compaction wave (313 m/s), the accelerating detonation wave in compacted material, and the detonation in the undisturbed bed. The piston positions at the times of radiographs are also shown, along with an extrapolation. Figure 7(b) is an expanded plot of the ionization pin data that more clearly shows the run to detonation and full-velocity detonation in the compacted bed (6.2 km/s). The change to detonation velocity in the original bed (6.4 km/s) occurs after the compaction wave is overtaken. These features correspond to the lines denoted as c, G, D_1, D_2, and p in Figure 4.

In Shot No. E-5586, three light fibers were added to the usual pins and radiographs. The 0.3-mm-diameter Si fibers were inserted through the steel tube wall until flush with the HMX bed. The light transmitted by the fibers was converted to voltage using Optelecom Series 3200R Analog Fiber Optic Receivers. The signals recorded from the three fibers, along with their positions relative to the piston at rest, are shown in Figure 8. The signals are shifted 0.2 V from one another on the ordinate to prevent overlap at later times. The most striking feature of the ensemble is the qualitative difference of the third signal (x = 42.6 mm) from the first two. Radiographs show that the third fiber was positioned in the plug region (between G and g in Figures 3 and 4), and the others were below the plug's lowest extent . The salient features of the first two fibers (x = 23.5 and 33.0 mm) are the fast rise and the "spike" of the initial edge, and the constant level until times long after detonation began at about 230 μs. The third signal is characterized by a low-level "toe" starting at 222 μs, a more slowly rising signal to a point of inflection, and a final signal level 0.4 V higher than the first two. Figure 9 is an expansion of the abscissa showing the relative slopes of the signal's leading edges. The slope of the signal from x = 33 mm is significantly less than that from x = 23.5 mm. These results are taken as evidence of a burn front b (shown in Figures 3 and 4) with nearly constant conditions behind. The changing slope as a function of position may

indicate the edge of the burn front is becoming somewhat more diffuse as it progresses through the 90% TMD bed.

All the data obtained for Shot No. E-5586 are projected in the x-t plane in Figure 10. The light signals are represented by dashed lines with symbols at each end that cover their temporal extent. The 42.6-mm signal has three symbols on the line noting the leading edge of the "toe", the point of inflection, and the cessation of the signal. The extent of the plug in the distance axis is indicated. The times for the flash radiographs are labeled by the arrows at X1, X2, and X3. Figure 11 shows the most interesting portion of Figure 10. In this diagram, the two ionization pins at about 202 and 212 μs are connected by line segments that also intersect the "toe" of the third light signal. This is a reasonable assumption because the ionization pins report at the first appearance of conductivity, and the first light emission indicates the presence of reaction, which also must be accompanied by conductivity. This trajectory is the plug top G, as in Figure 4.

The front edges of the light signals from the first two fibers are connected by a line that is extrapolated to shorter times. The previously discussed temporal profile of these light signals is the evidence for a well-defined burn front. We postulate that when the burn front intersects with the bottom of the plug is an important event in the deflagration-to-detonation transition. After this time, the plug is subjected to the full pressure of the burning HMX without benefit of any layer of unburnt material to reduce the stress. This interface at the plug bottom g behaves like an accelerating piston, and the resultant shock G is driven at an ever-increasing velocity into the compacted bed. When the velocity of G and the pressure generated are high enough, the HMX bed will transit to detonation in a manner analogous to the mechanism of heterogeneous initiation. [2]

There is evidence for the initial bed collapse and formation of the plug (Figure 3d) in the second radiograph of Shot No. E-5586. The density-vs-distance plot derived from these data is shown in Figure 12. A small region of density greater than the 90% TMD compaction is indicated near 30 mm. We thus infer that initial bed collapse occurs before the extensive growth of the plug. A coalescence of stress waves generated by the accelerating burn front (see Figure 4) can exceed the strength of the HMX bed in this region, thus forming the plug a considerable time before its rapid growth. The time and position of this initial collapse are indicated in Figure 11.

All of the experiments performed in this study have not behaved as simply as those discussed in the preceding section. Figure 13 reproduces the radiographs from Shot No. F-5408. In the second dynamic radiograph are two regions of closely spaced foils indicating the formation of two plugs. Analyses of the two dynamic radiographs are given in Figures 14 and 15. The first radiograph shows a burning region from the piston to about 46 mm, followed by a 100% TMD plug from 53 to 65 mm, followed by another 90% TMD region to about 86 mm. The second radiograph, taken after transition to detonation, shows the residuals of two separate plugs, near 60 mm and 87 mm.

The x-ray and pin data for Shot No. F-5408 are presented in the x-t plane in Figure 16. Note in the figure that detonation failed to occur after formation of the first plug, but it did occur after the second plug. An x-t schematic for this situation is presented in Figure 17. The details of the various wave interactions are analogous to those presented in Figure 4, except that detonation fails to occur after the formation of the first plug. The pressure developed at the shock G is never sufficient to initiate the compact HMX. Thus, when G overtakes the first compaction wave c, there is not enough impulse to initiate the original 65% TMD bed, and the plug (1) acts like a second piston by launching a second compaction wave c'. The events from burn front development to plug formation are then repeated further up the tube. If pressures along G' are sufficiently high, transition to detonation will occur. There is no *a priori* reason for detonation to occur after the second plug. Situations are easily envisioned where consecutive plug formation might continue indefinitely. Indeed, Shot No. B-9088, whose radiographs are shown in Figure 18, exhibits three, and possibly four plugs. This experiment exhibited unusual behavior in that the compaction wave traveled the entire length of the tube, where it reflected off a steel plug. Plug formation and eventually detonation occurred from top to bottom. The analysis of the third dynamic radiograph is presented in Figure 19. It shows the detonation (retonation?) front at 85 mm, followed by the residuals of three or four plugs at 93, 146, 170, and (maybe) 185 mm.

CONCLUSION

Detailed analysis of radiographic and pin data for seven steel tubes packed with granulated HMX has led to a picture of the deflagration-to-detonation transition that

requires a combustion-driven plug to be formed in compacted material. The material may be directly shock initiated to detonation, may require interaction of the plug with the compaction wave to initiate detonation, or may initiate burning and form an additional compaction wave. This last case may then continue on to form another plug that might initiate detonation, or the plug-deflagration cycle may be repeated.

REFERENCES

1. A. W. Campbell, "Deflagration-to-Detonation Transition in Granular HMX," 1980 JANNAF Propulsion Systems Hazards Subcommittee Meeting, Monterey, California, March 1980, CPIA Publication 330, pp. 105-130. Los Alamos National Laboratory document LA-UR 80-2016.

2. A. W. Campbell, W. C. Davis, J. B. Ramsay, and J. R. Travis, "Shock Initiation of Solid Explosives," Phys. Fluids *4* (4), 511-521 (1961).

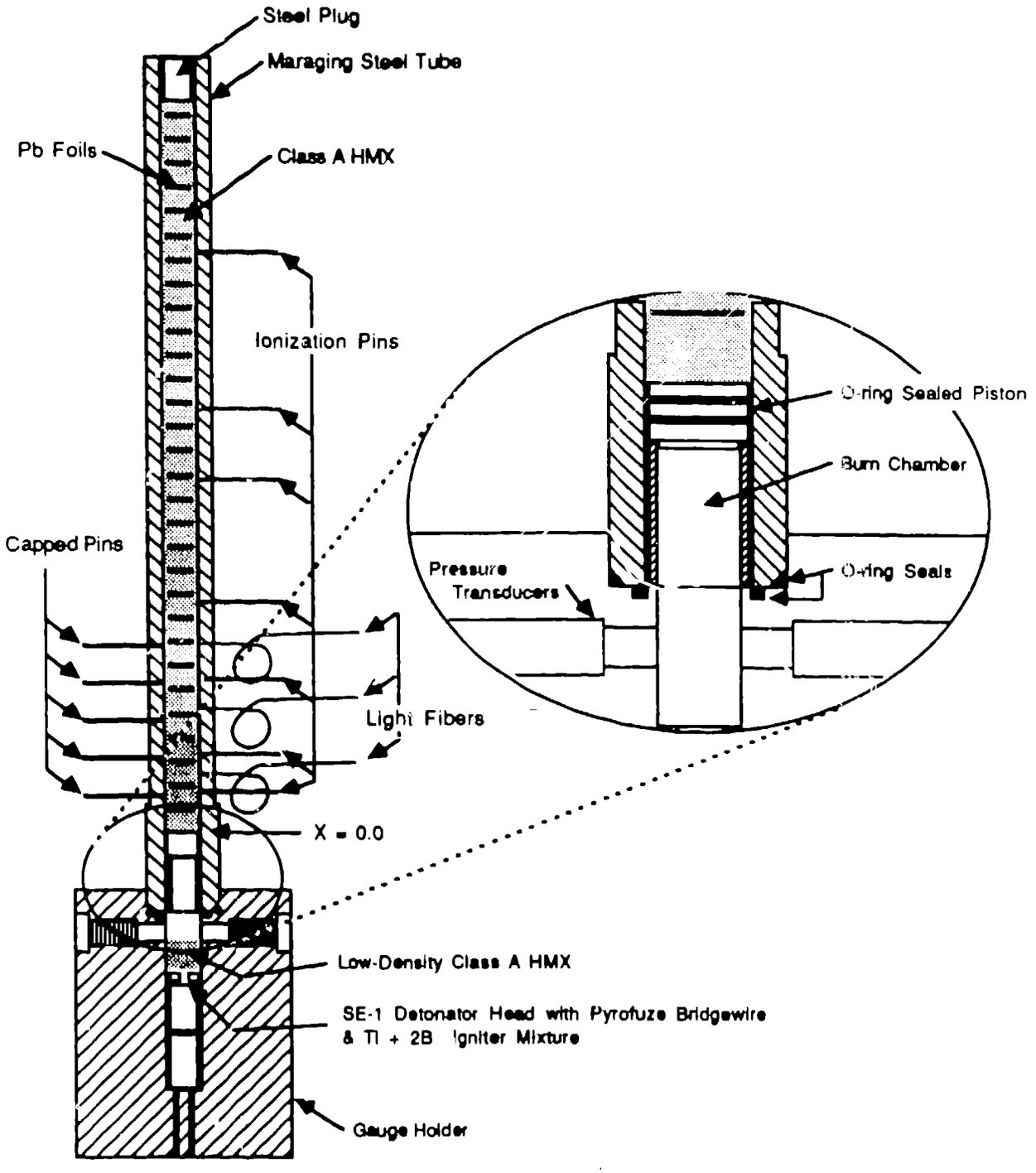

Fig. 1. Schematic of DDT Tube Experiments.

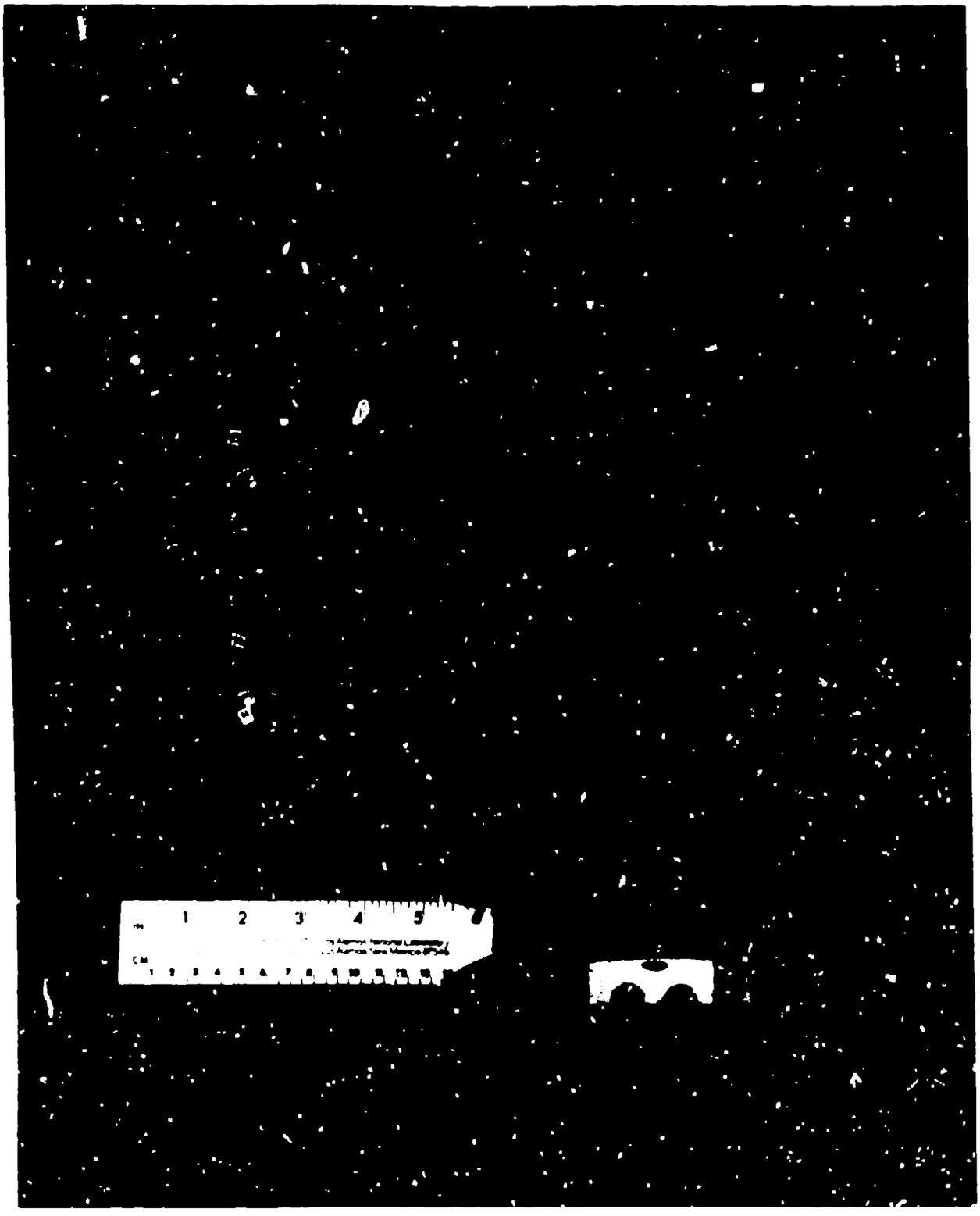

Fig. 2. Typical DDT tube.

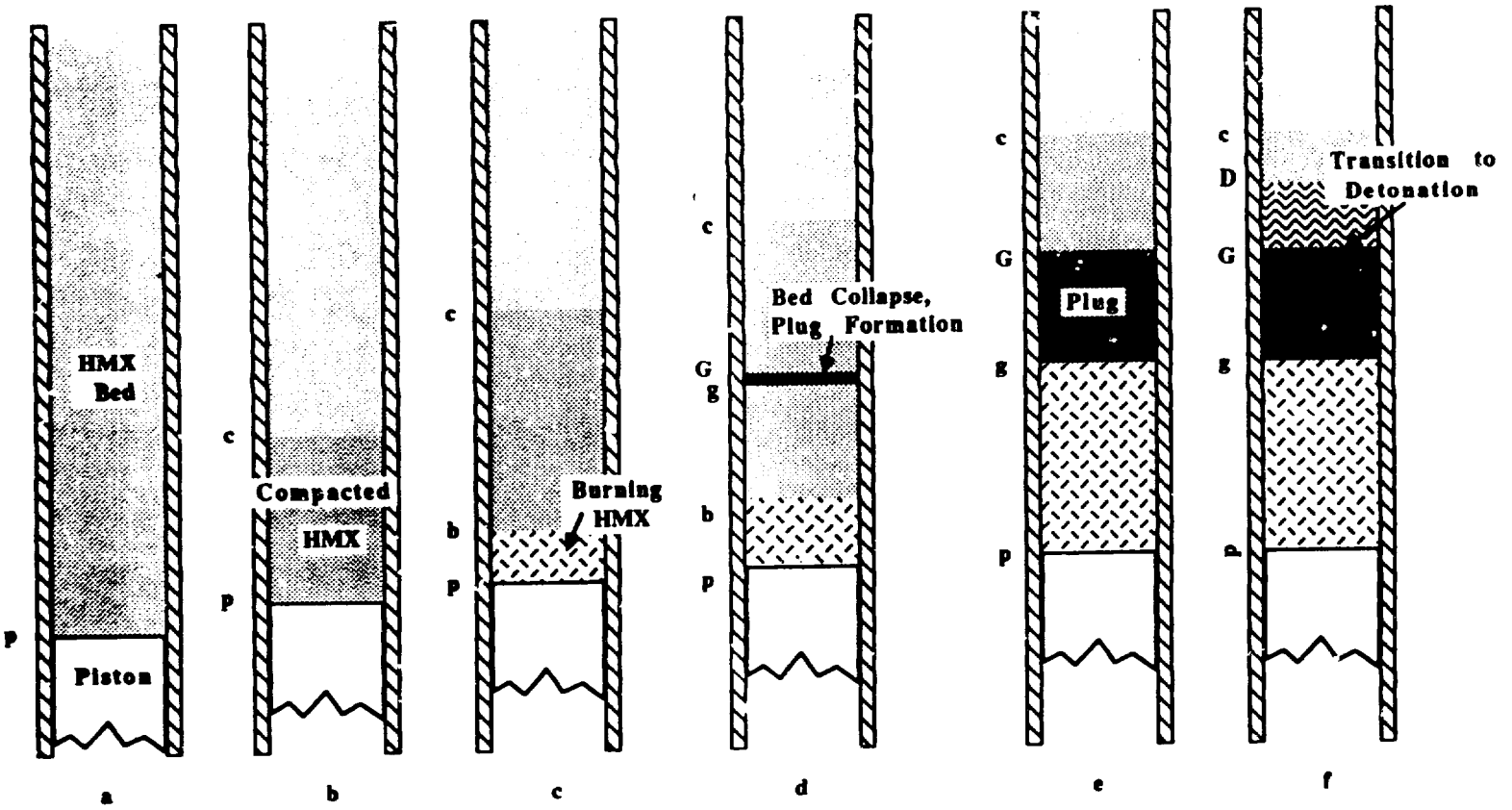

Fig. 3. Schematic Description of Deflagration-to-Detonation Transition in Granular HMX.

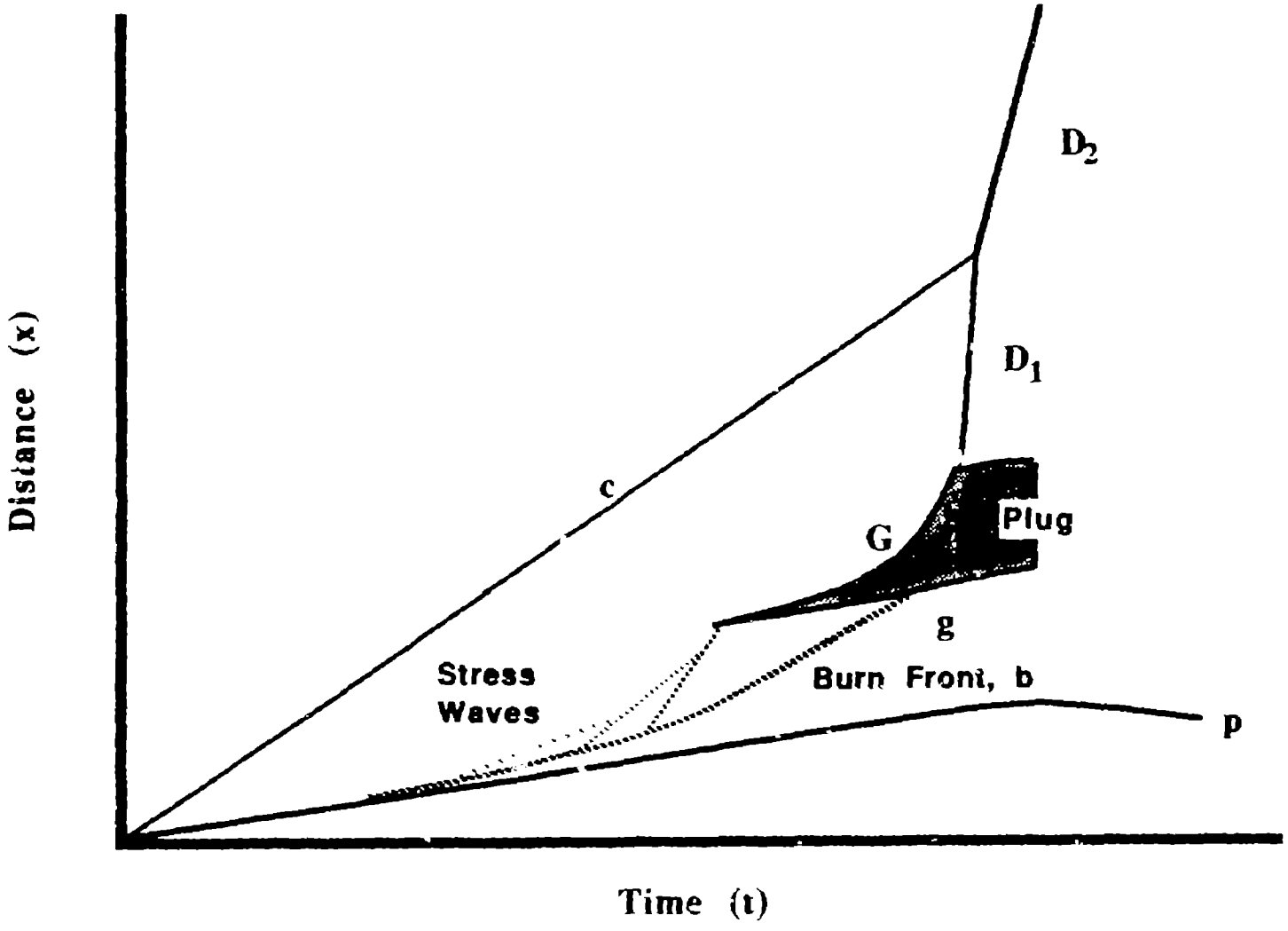

Fig. 4. Space-Time Representation of the Simple DDT Process.

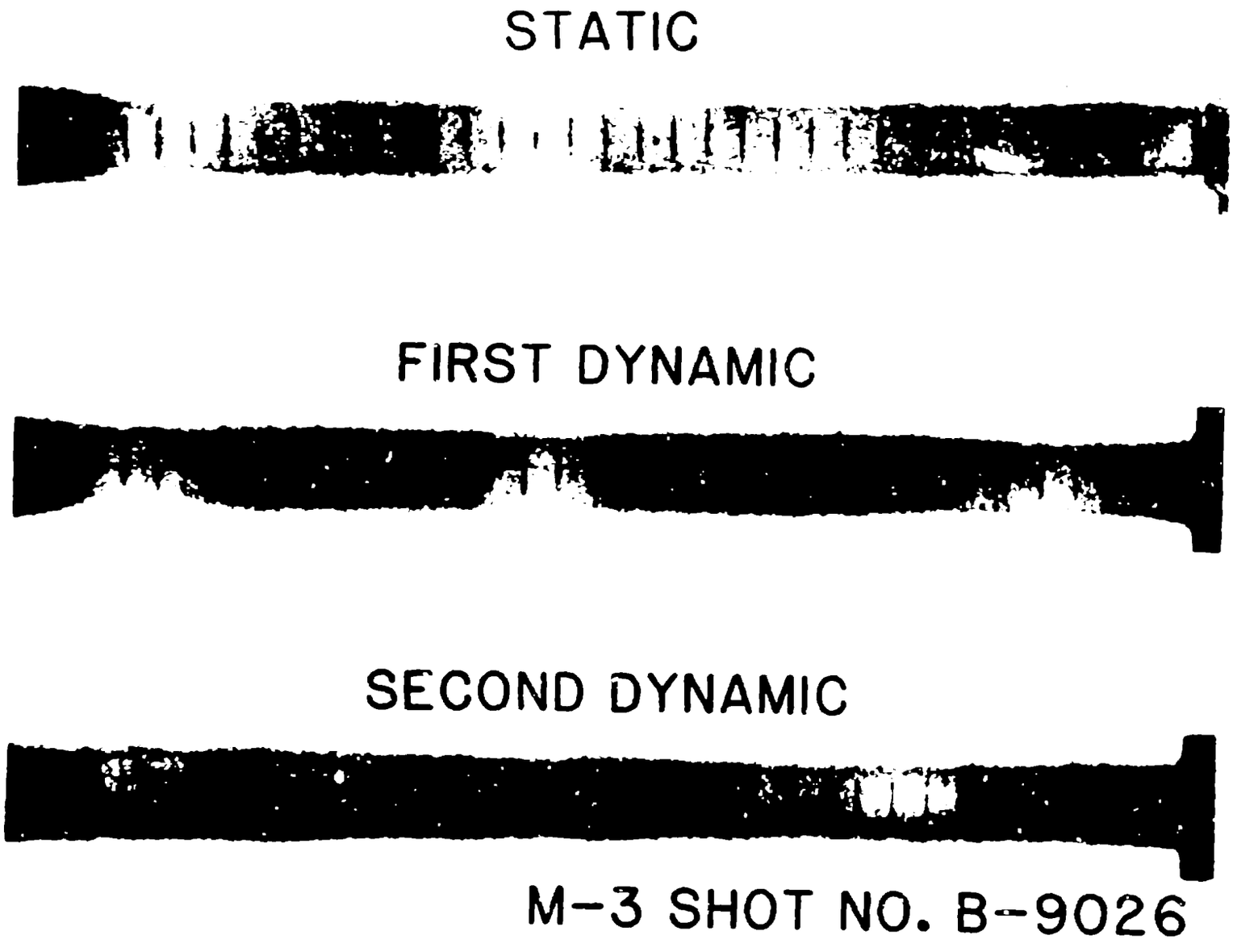

Fig. 5. Radiographic results.

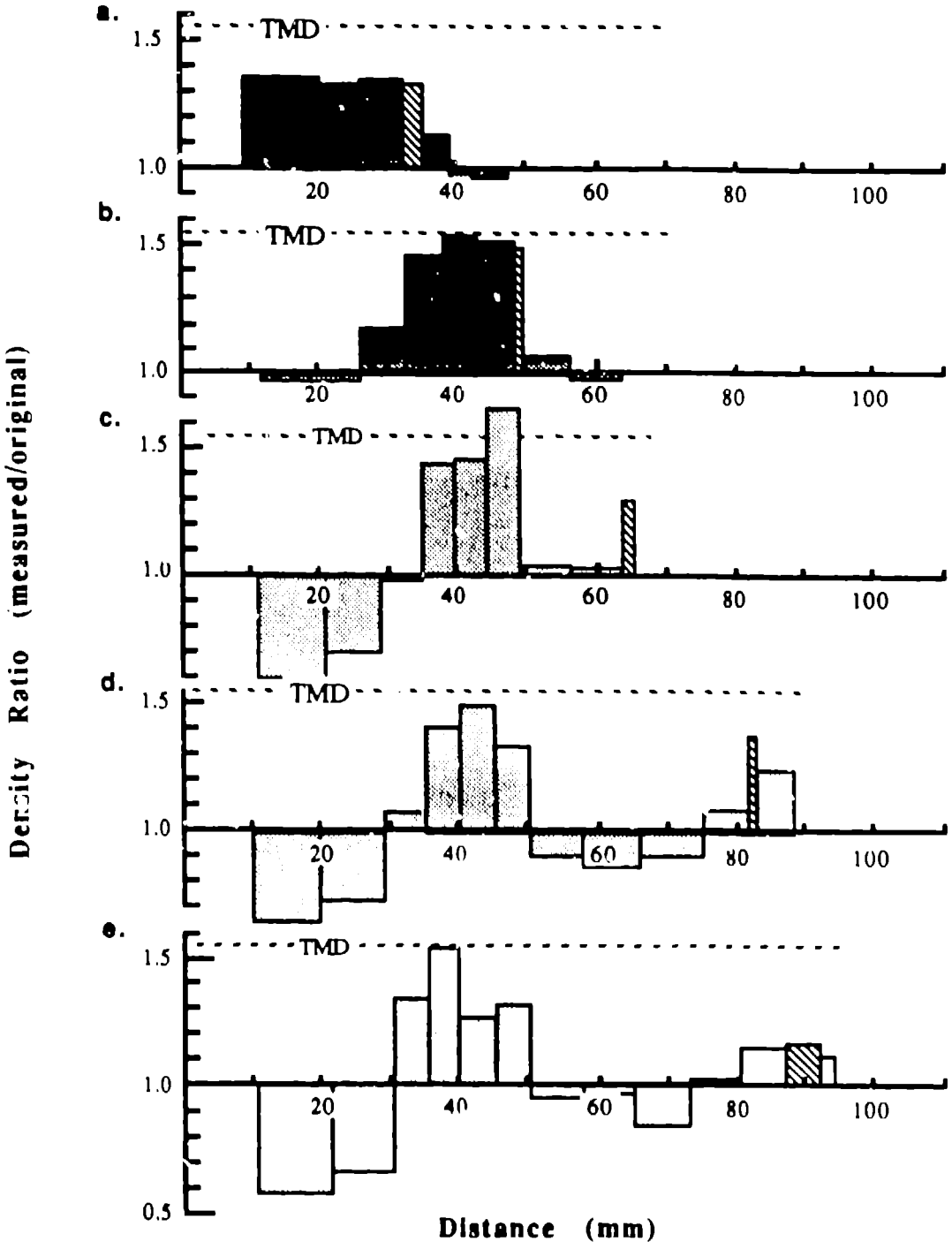

Fig. 6. Relative Density vs Position from Radiographs.

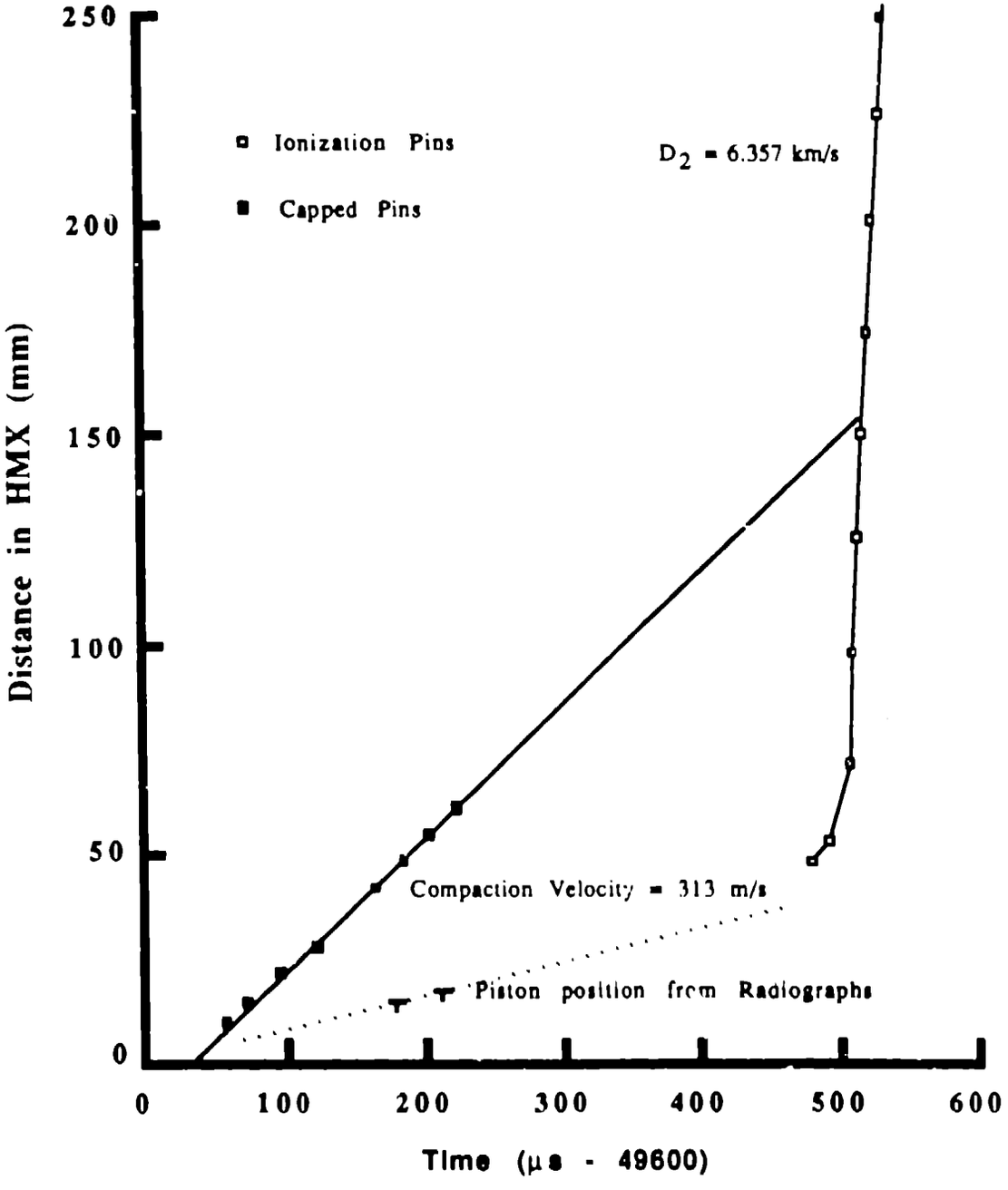

Fig. 7(a). Cap and Ion Pin Data for Shot No. B-9036.

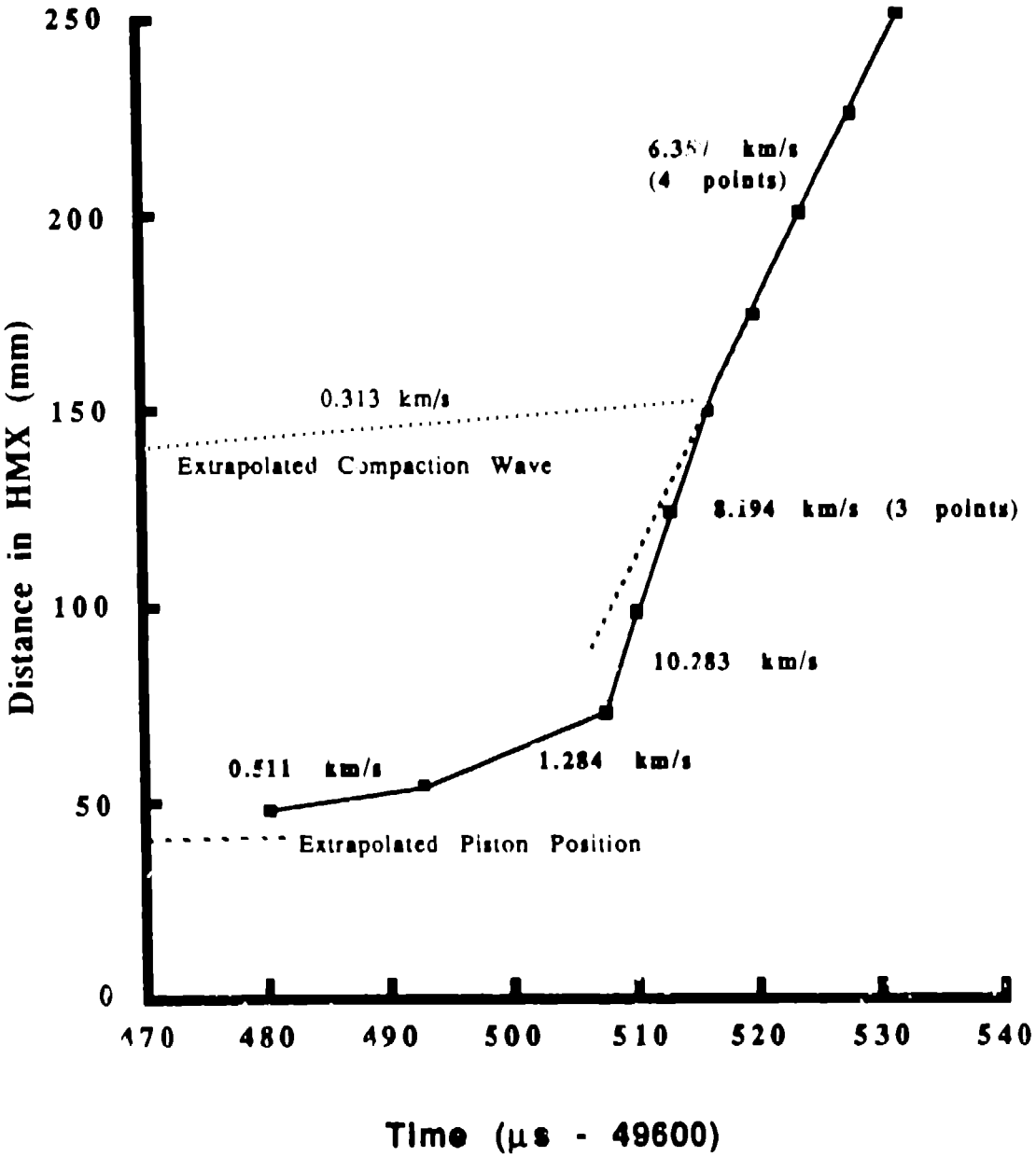

Fig. 7(b). Ion Pin Data for Shot No. B-9036.

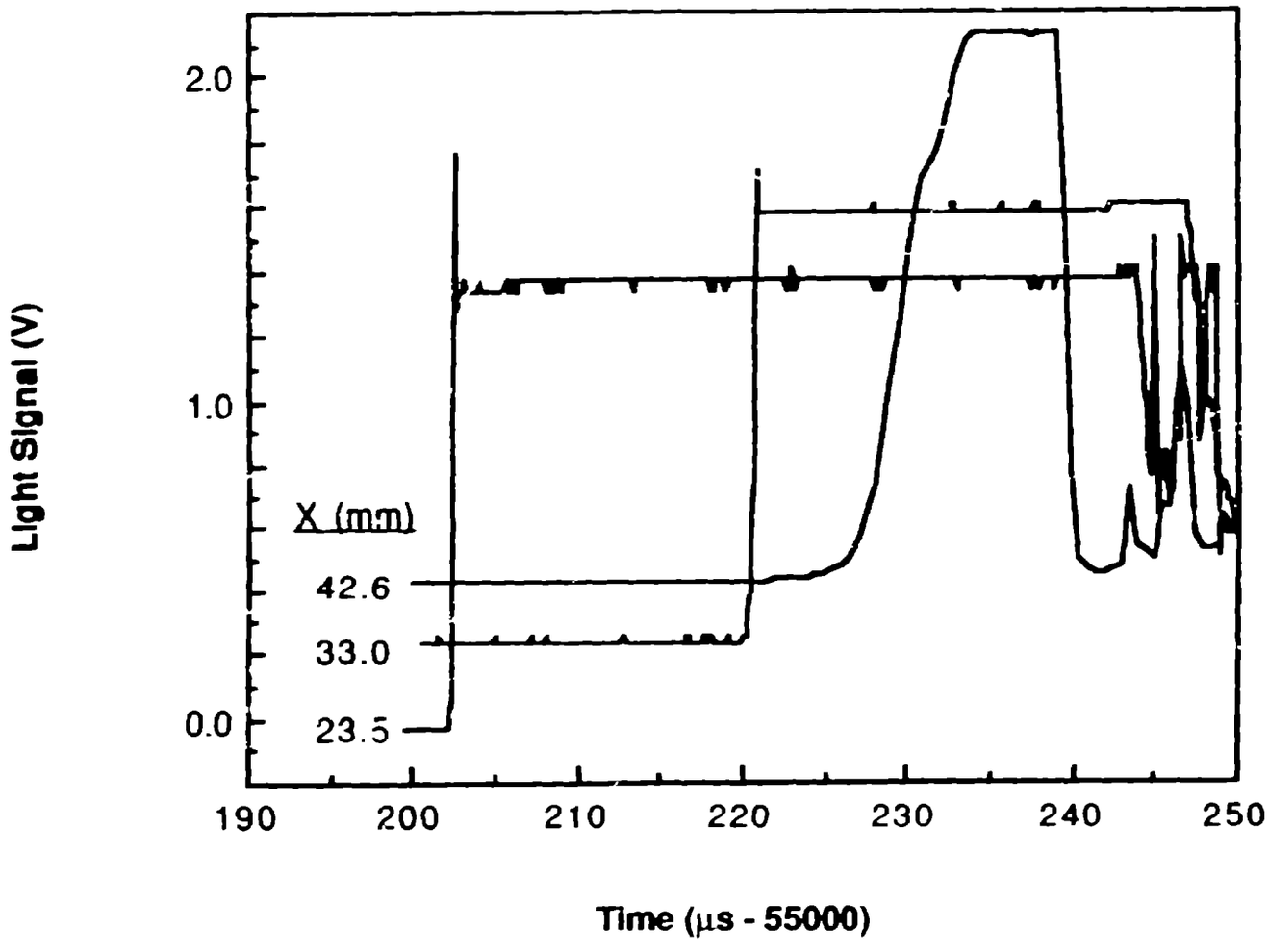

Fig. 8. Fiber-Optic Signals for Shot No. E-5586.

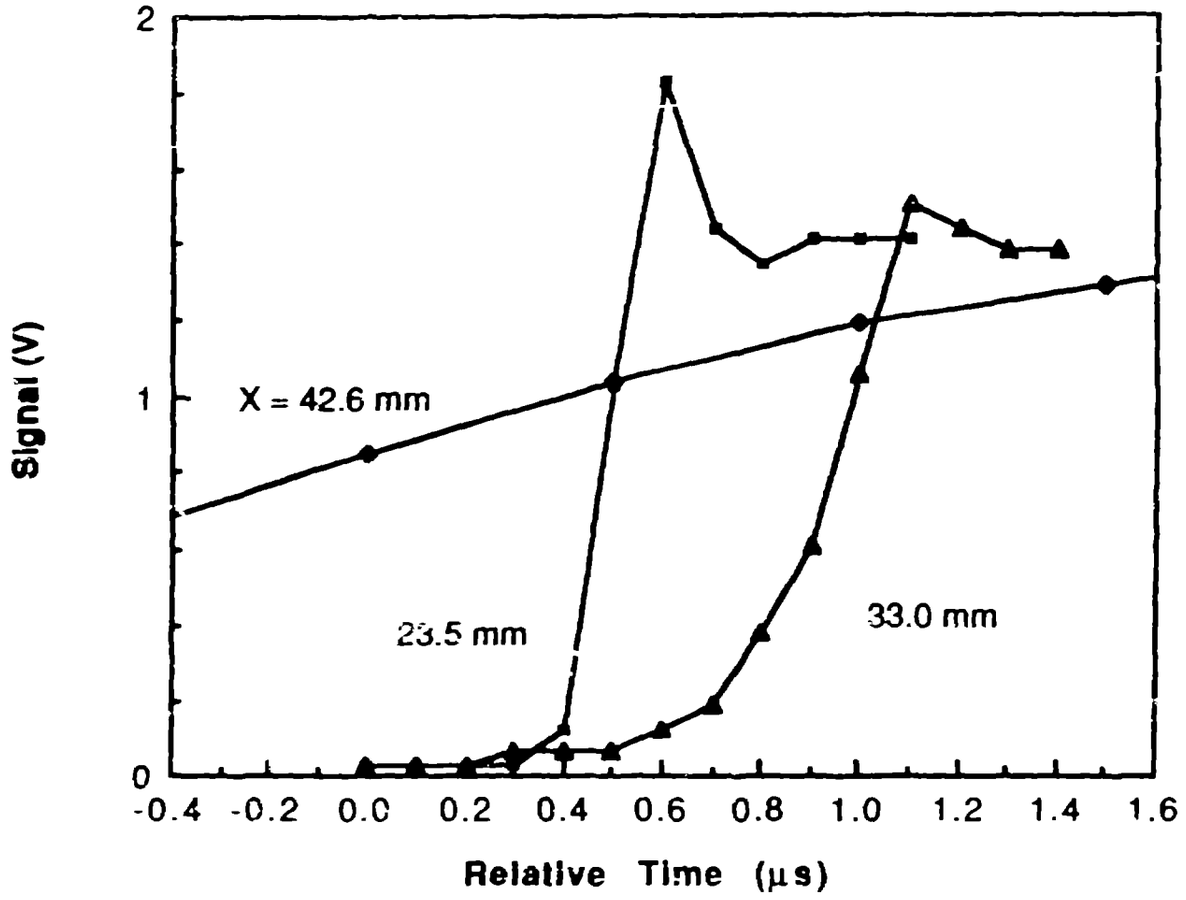

Fig. 9. Risetimes of Light Signals for Shot No. E-5586

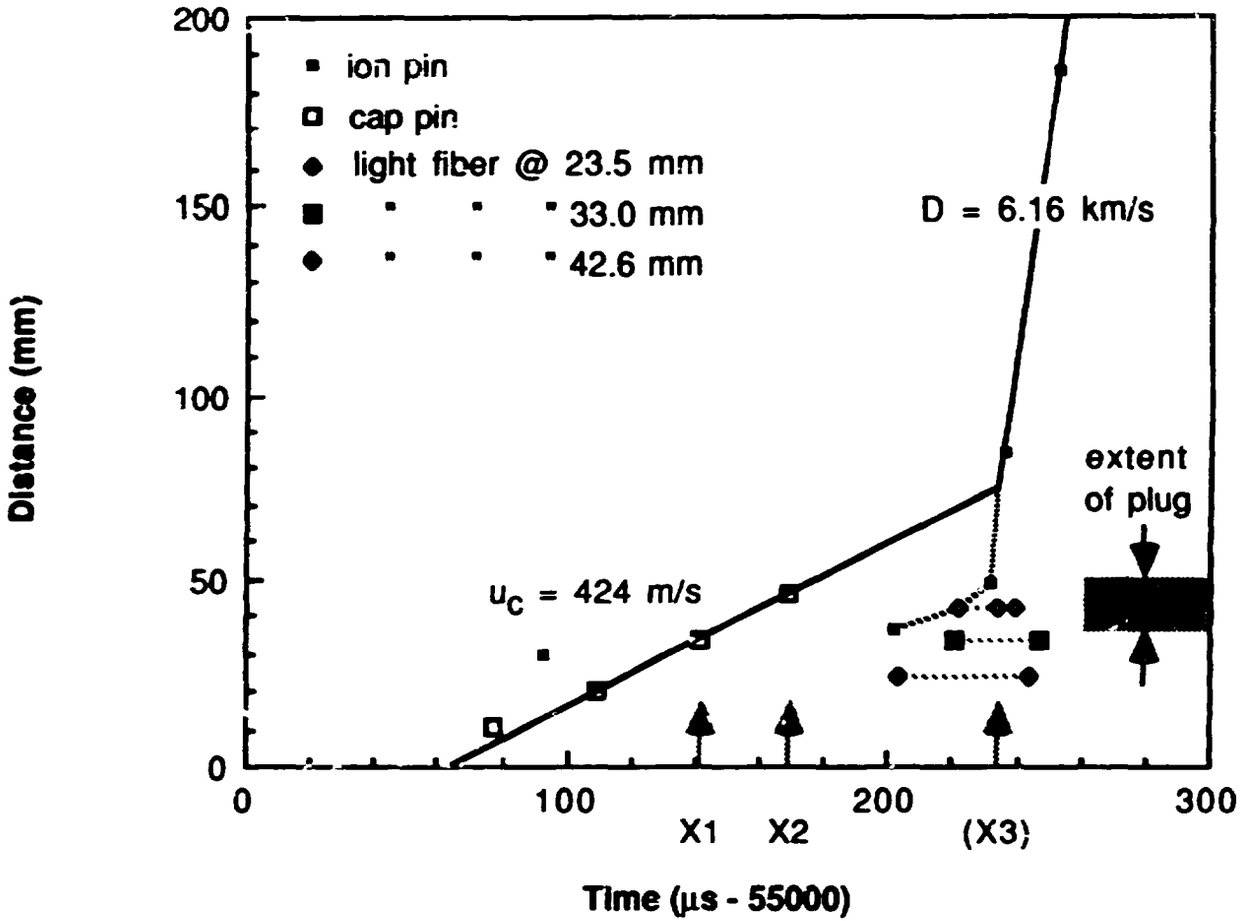

Fig. 10. Shot No. E-5586 Data from Pins, Light Fibers, and Radiographs.

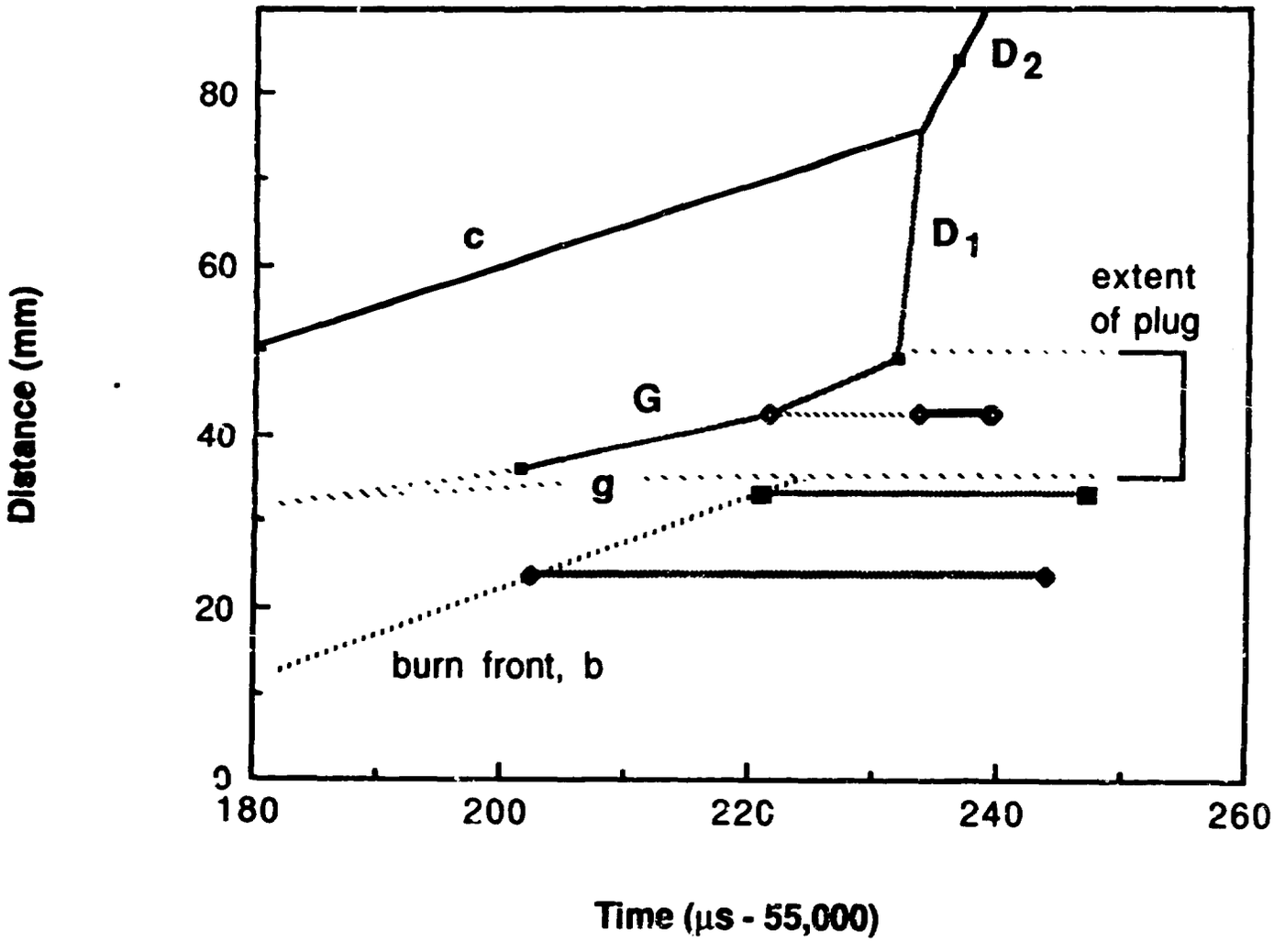

Fig. 11. Enlarged Detail of E-5586 Pin and Light Signals.

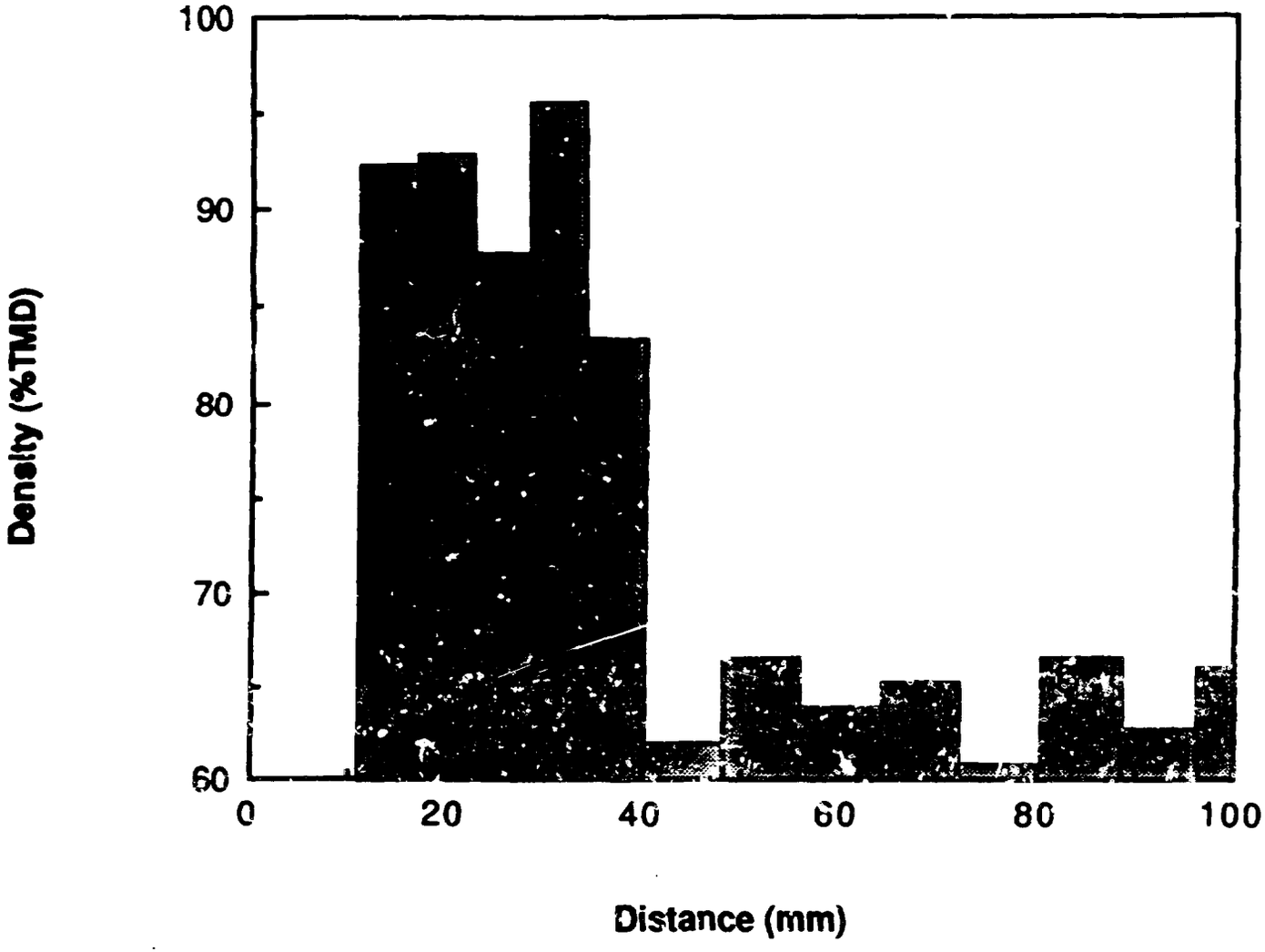

Fig. 12. Density vs Distance for Second Radiograph of Shot No. E-5586.

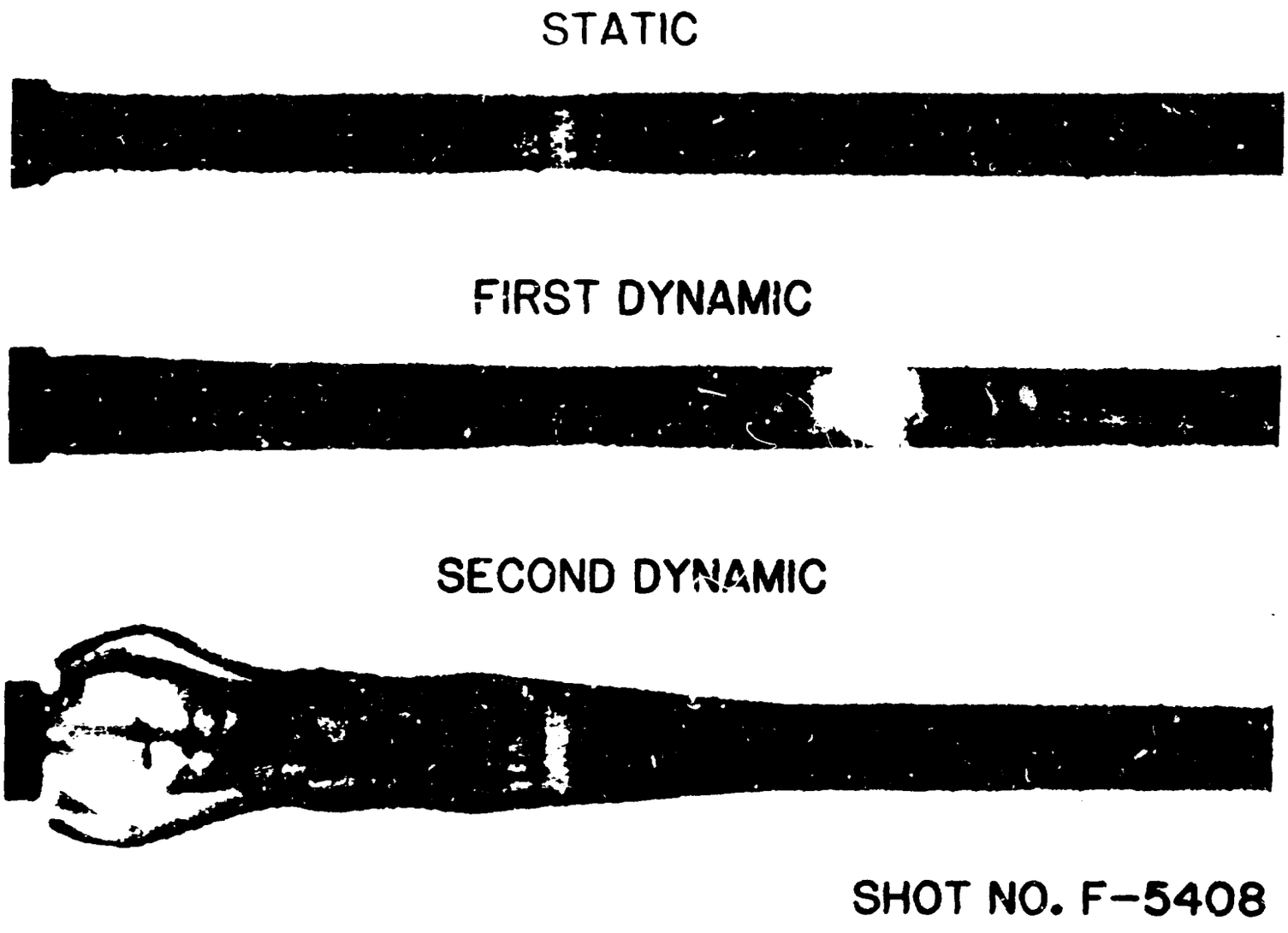

Fig. 13. Radiographic results.

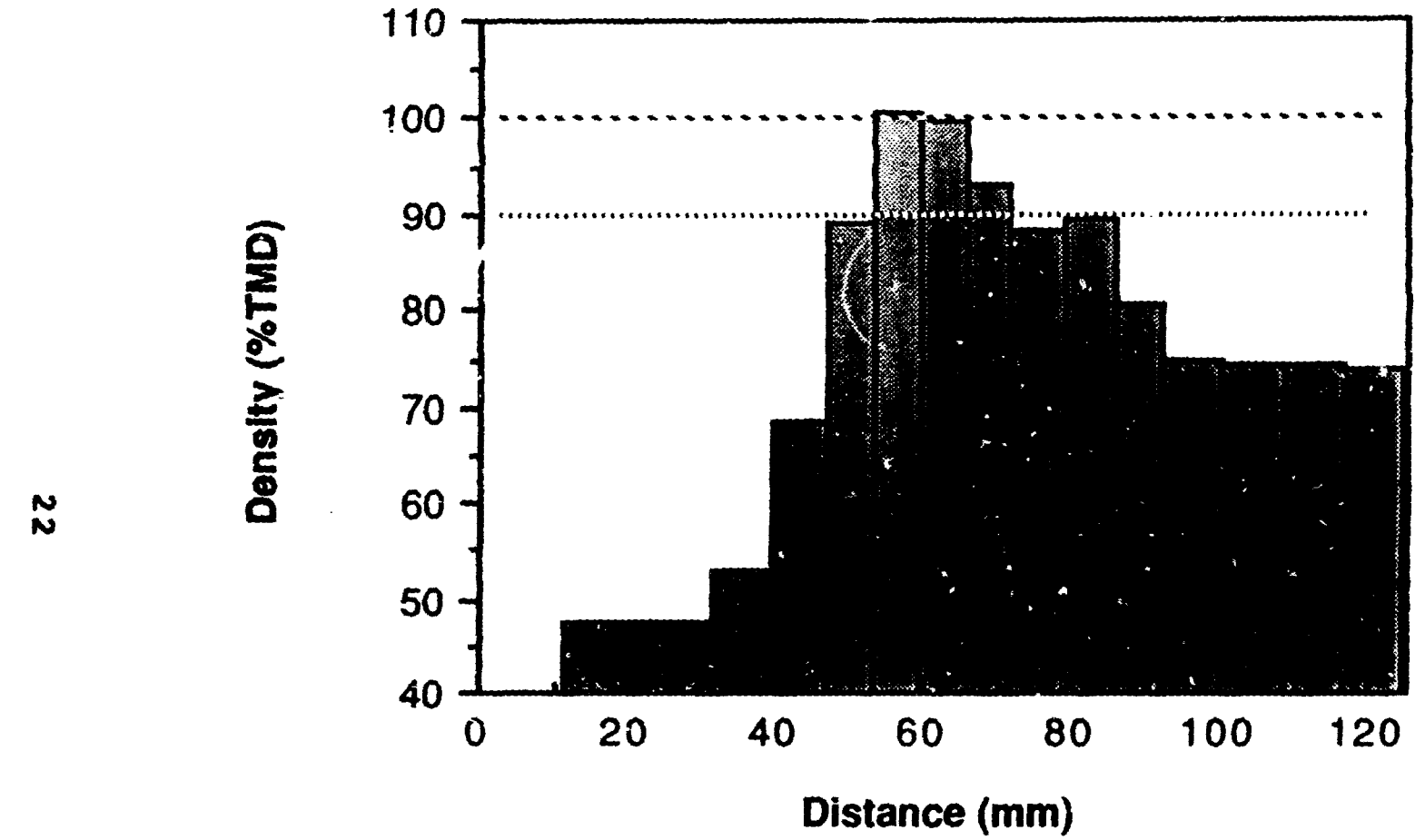

Fig. 14. Density vs Distance for First Radiograph of Shot No. F-5408.

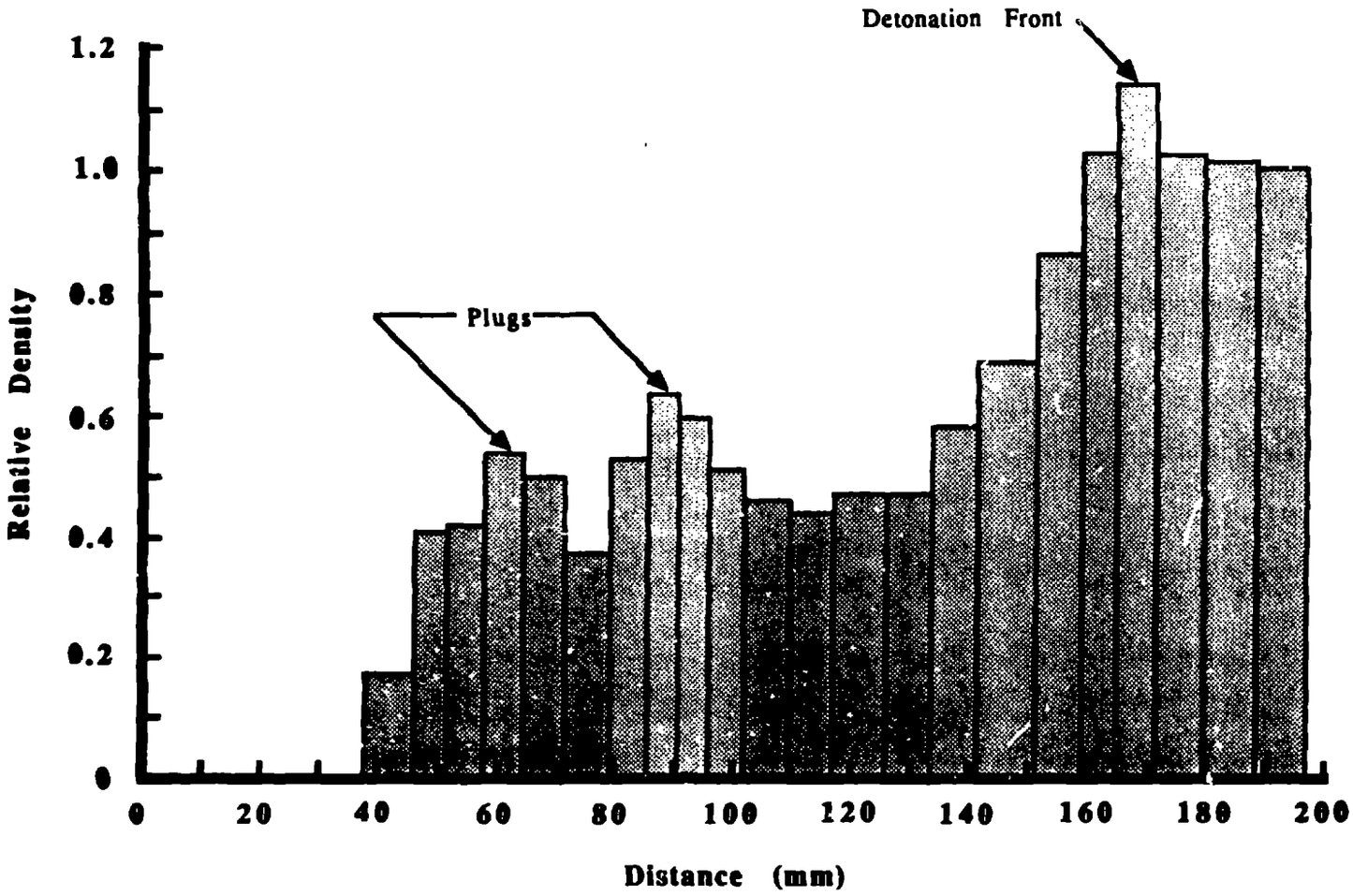

Fig. 15. Density vs Distance for Second Radiograph of Shot No. F-5408.

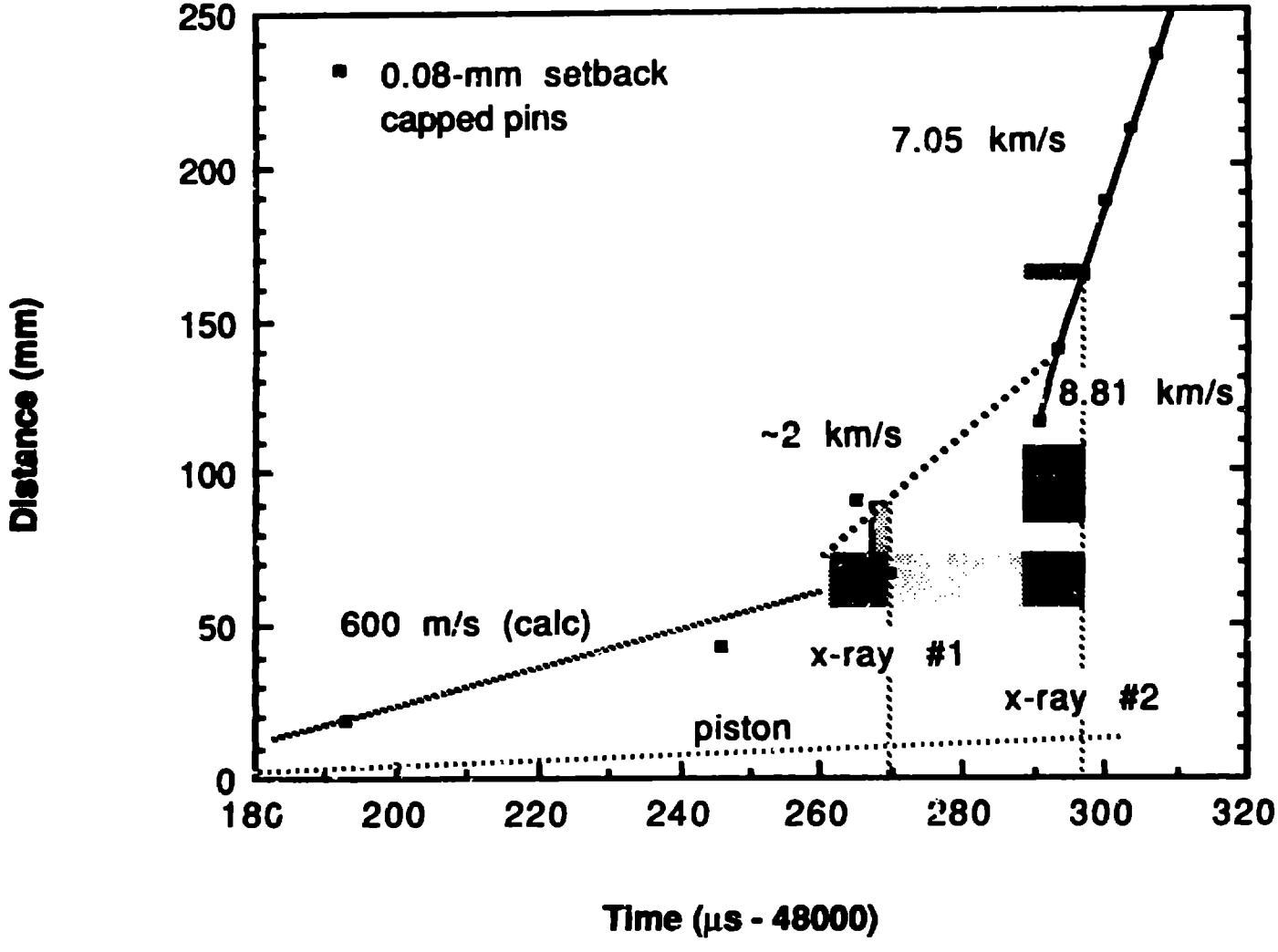

Fig. 16. Pin and Radiograph Data for Shot No. F-5408.

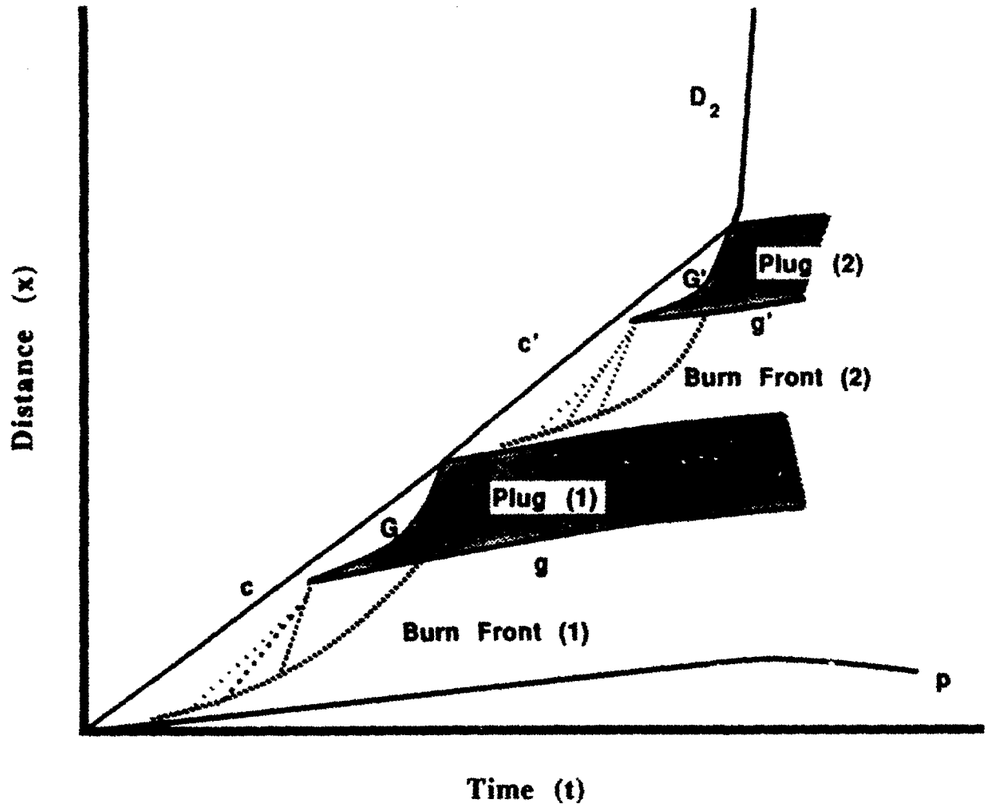

Fig. 17. Diagram of Consecutive Plug Formation in DDT Process.

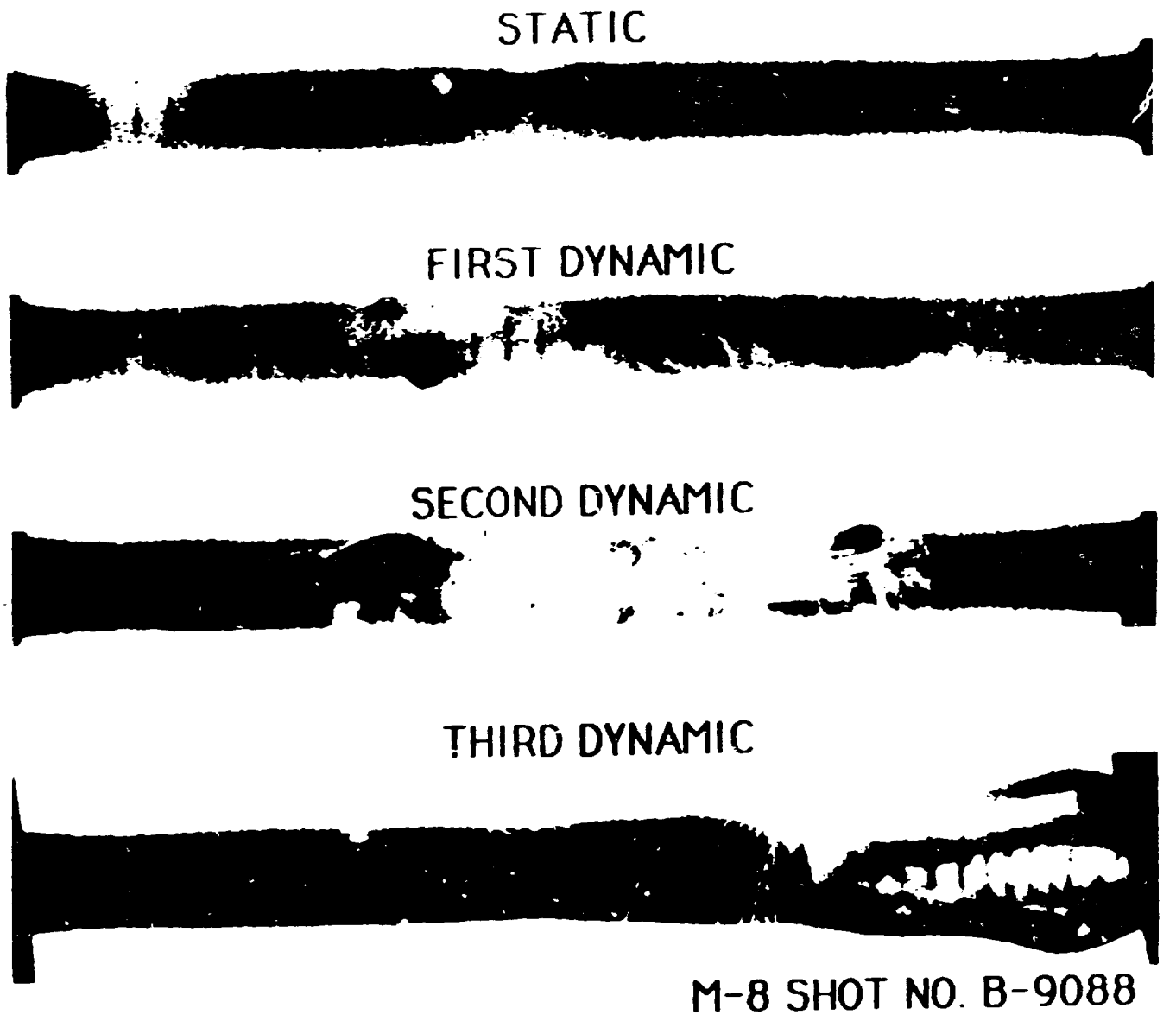

Fig. 18. Radiographic results.

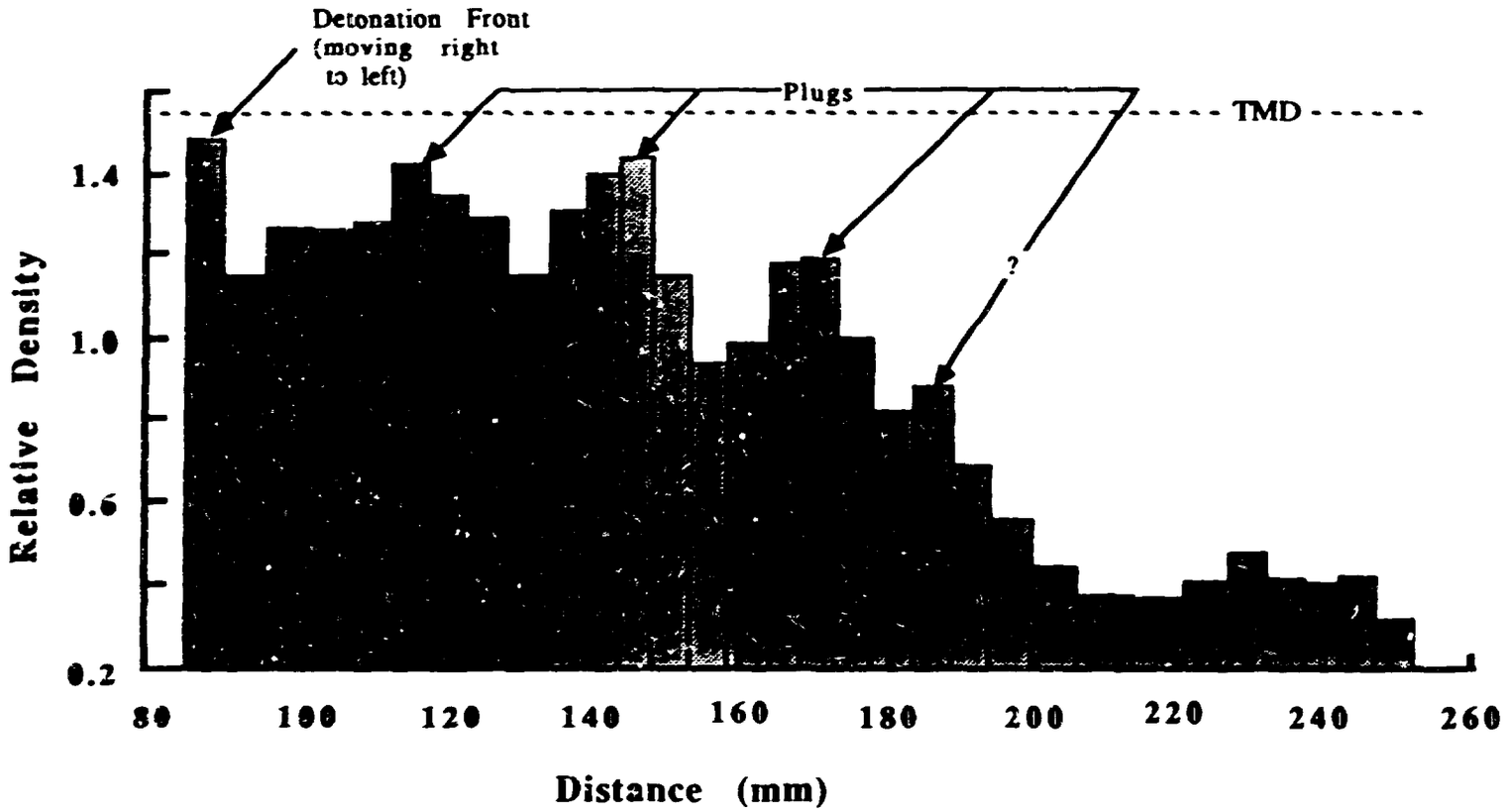

Fig. 19. Density vs Distance for Third Radiograph of Shot No. B-9088.